Secrecy Capacity of IRS-Assisted Terahertz Wireless Communications With Pointing Errors

DOI:
10.1109/LCOMM.2023.3246169

Document Version
Accepted author manuscript

Secrecy Capacity of IRS-Assisted Terahertz Wireless Communications With Pointing Errors

Ahmad Massud Tota Khel, and Khairi Ashour Hamdi, *Senior Member, IEEE*

***Abstract*—This letter considers an intelligent reflecting surface (IRS)-assisted terahertz (THz) communication system in the presence of an arbitrary number of colluding/non-colluding eavesdroppers (Eves). Although the instantaneous channel state information (CSI) of the legitimate user (Bob) is assumed to be available, the IRS with discrete phase shifters cannot achieve optimal phase shifts, and thus Bob suffers from phase shift quantization errors. By taking into account the availability of the statistical CSI of Eves, pointing errors caused by highly-directional THz antennas, and the phase shift quantization errors, new expressions for the secrecy capacity in both cases of Eves are derived. The accuracy of the expressions is then verified by Monte-Carlo simulations. These expressions are used to investigate the impacts of pointing errors and quantization errors on the physical layer security of IRS-assisted THz systems in the presence of colluding and non-colluding Eves.**

***Index Terms*—Colluding eavesdroppers, intelligent reflecting surface, non-colluding eavesdroppers, pointing errors, terahertz.**

I. Introduction

TERAHERTZ (THz) technology is a promising solution to address the ultra-high data rates requirements of next generation communication systems. Moreover, due to the highly-directional THz antennas, the signals with narrow beam-widths improve the robustness of THz systems against eavesdropping attacks [1]. However, the deployment of such antennas leads to beam misalignment or pointing errors (PE) [2]. Furthermore, the molecular absorption due to very small wavelengths at THz band leads to energy absorption and higher path-losses [2]. In addition, THz systems severely suffer from channel attenuation due to non-line-of-sight (NLOS) and blockages [1], which impacts the physical layer security (PLS) as the eavesdroppers (Eves) may have LOS and can be located in close proximity to the transmitter (Alice). On the other hand, intelligent reflecting surface (IRS) is another promising technology having an array of reflecting elements (REs), which intelligently manipulates the scattering properties of its REs and forms strong beams towards a desired destination [1], [3]. Therefore, the integration of THz and IRS technologies significantly improves the PLS and overall system performance [1].

The authors in [3] and [4] have respectively analyzed the secrecy outage and capacity performance of IRS-assisted conventional wireless systems in the presence of a single Eve. In [5], the secrecy capacity of IRS-assisted conventional wireless systems in the presence of non-colluding Eves has been studied. It is noteworthy that the aforementioned works are based on the assumption of optimal IRS phase shifts. However, due to inherent limitations in the IRS hardware, this assumption is impractical and unrealistic [6]. On the other hand, a limited number of works on the optimization and secrecy performance maximization of IRS-assisted THz communications has been reported [7]–[9]. In more details, the authors in [7], [8] and [9] have carried out beamforming design for secrecy rate maximization of IRS-assisted THz communications in the presence of a single Eve and non-colluding Eves, respectively. However, they have ignored the impacts of PE caused by the highly-directional THz antennas. To the best of our knowledge, in the current open literature, no work has been reported on the secrecy performance analysis of IRS-assisted THz communications in the presence of PE and non-ideal phase shifts. Furthermore, the impacts of colluding and non-colluding Eves on the secrecy capacity of IRS-assisted THz communications have not been compared and studied.

Motivated by the considerations above, in this letter, we consider an IRS-assisted THz communication system, where an arbitrary number of colluding/non-colluding Eves attempt to intercept the Alice-legitimate user (Bob) information. In the case of colluding eavesdropping, the Eves are cooperative, and thus the maximum ratio combining (MRC) technique is used. Whereas, in the case of non-colluding, by considering the Eve with the strongest signal-to-noise ratio (SNR), the selection combining (SC) technique is used. Moreover, the IRS is assumed to be equipped with discrete phase shifters, where the phases cannot be perfectly aligned. Therefore, by considering the phase shift quantization errors, PE and the large-scale path-loss along with the molecular absorption losses, new expressions for the secrecy capacity are extracted. The accuracy of the expressions is validated by numerical and simulation results. The results show the significant impacts of PE, quantization errors and colluding Eves on the secrecy capacity. It is also shown that the asymptotic secrecy capacity reaches a limit, which is scaled with the number of REs.

The rest of this letter is organized as follows. The system model, closed-form expressions, and the results are presented in Section II, Section III and Section IV, respectively. Finally, a conclusion of the letter is provided in Section V.

II. System Model

We consider an IRS-assisted THz communication system, where due to blockages, it is assumed that the Alice-Bob and Alice-Eves direct links do not exist. However, Alice utilizes an N-element IRS to securely communicate with Bob. On

Manuscript received xxxxx xx, 2023; revised xxxxxx xx, 2023; accepted xxxxxxx xx, 2023. Date of publication xxxxxx xx, 2023; date of current version xxxxxxx xx, 2023. The associate editor coordinating the review of this letter and approving it for publication was xxxxxxx xxxxxxxx. *(Corresponding author: Ahmad Massud Tota Khel.)*

The authors are with the Department of Electrical and Electronic Engineering, The University of Manchester, Manchester M13 9PL, United Kingdom (e-mail: ahmadmassud.totakhel@postgrad.manchester.ac.uk; k.hamdi@manchester.ac.uk).

Digital Object Identifier xx.xxxx/COML.2023.xxxxxxx

the other hand, M Eves attempt to establish communication through the IRS to overhear the Alice-Bob information. It is also assumed that due to severe path-loss, molecular absorption and PE, the power of the signals reflected by the IRS more than once is negligible. The Alice-IRS, IRS-Bob and IRS-Eves fading channel coefficients are respectively denoted by $h_i \sim \mathcal{CN}(\mu_{h_i}, \sigma^2_{h_i})$, $g_i \sim \mathcal{CN}(\mu_{g_i}, \sigma^2_{g_i})$ and $\mathcal{E}_{i,m} \sim \mathcal{CN}(\mu_{i,m}, \sigma^2_{i,m})$ $\forall i = 1, \ldots, N$ and $\forall m = 1, \ldots, M$, which are complex Gaussian (CG) random variables (RVs). Moreover, the large-scale path-losses along with the molecular absorption for Bob and Eves are respectively written as [10]

$$\alpha_b = \sqrt{\frac{G_t G_b}{64\pi^3}} \frac{c}{f d_1 d_2} \exp\left(-\frac{\kappa\left(f\right)\left(d_1 + d_2\right)}{2}\right), \quad (1)$$

$$\alpha_m = \sqrt{\frac{G_t G_m}{64\pi^3}} \frac{c}{f d_1 d_{2,m}} \exp\left(-\frac{\kappa\left(f\right)\left(d_1 + d_{2,m}\right)}{2}\right), \quad (2)$$

where G_t, G_b and G_m are respectively the antenna gains of Alice, Bob and Eves, c is the speed of light, f is the carrier frequency, and d_1, d_2 and $d_{2,m}$ are the Alice-IRS, IRS-Bob, and IRS-Eves distances, respectively. Furthermore, $\kappa\left(f\right)$ represents the molecular absorption coefficient, where it can be obtained through the high resolution transmission (HITRAN) database [2], [11]. It is to note that for 275-400 GHz frequency band, it can be accurately calculated as [2]

$$\begin{aligned}\kappa\left(f\right) =& \frac{\mathcal{A}(\varrho)}{\mathcal{B}(\varrho) + \left(\frac{f}{100c} - \mathcal{C}_1\right)^2} + \frac{\mathcal{C}(\varrho)}{\mathcal{D}(\varrho) + \left(\frac{f}{100c} - \mathcal{C}_2\right)^2} \\ &+ \rho_1 f^3 + \rho_2 f^2 + \rho_3 f + \rho_4, \end{aligned} \quad (3)$$

where $\mathcal{A}(\varrho) = 0.2205\varrho(0.1303\varrho + 0.0294)$, $\mathcal{B}(\varrho) = (0.4093\varrho + 0.0925)^2$, $\mathcal{C}(\varrho) = 2.014\varrho(0.1702\varrho + 0.0303)$, $\mathcal{D}(\varrho) = (0.537\varrho + 0.0956)^2$, $\mathcal{C}_1 = 10.835\text{cm}^{-1}$, $\mathcal{C}_2 = 12.664\text{cm}^{-1}$, $\rho_1 = 5.54 \times 10^{-37}\text{Hz}^{-3}$, $\rho_2 = -3.94 \times 10^{-25}\text{Hz}^{-2}$, $\rho_3 = 9.06 \times 10^{-14}\text{Hz}^{-1}$, $\rho_4 = -6.36 \times 10^{-3}$, and ϱ is calculated based on the Buck's equations as [11]

$$\varrho = \phi\left(\frac{0.06116}{\rho} + \frac{2.1148}{10^7}\right)\exp\left(\frac{17.502T}{240.97 + T}\right), \quad (4)$$

where ϕ, ρ and T represent the relative humidity, the atmospheric pressure and the temperature, respectively.

In addition, let β and β_m respectively represent the PE for Bob and Eves, using [2, Eq. (22)], their probability density functions (PDFs) are written as (5) and (6), respectively.

$$f_\beta\left(\vartheta\right) = \xi\varphi^{-\xi}\vartheta^{\xi-1}, \quad 0 \le \vartheta \le \varphi, \quad (5)$$

$$f_{\beta_m}\left(\vartheta_m\right) = \xi_m\varphi_m^{-\xi_m}\vartheta_m^{\xi_m-1}, \quad 0 \le \vartheta_m \le \varphi_m, \quad (6)$$

where $\varphi = \left[\text{erf}(u)\right]^2$ and $\varphi_m = \left[\text{erf}(u_m)\right]^2$ are respectively the portions of power captured by Bob and Eves under perfect alignment conditions, $\xi = \frac{w^2}{4\sigma^2}$, $\xi_m = \frac{w_m^2}{4\sigma_m^2}$, w and w_m are the equivalent beam-widths and σ^2 and σ_m^2 are the variances of the PE displacement for the Alice-Bob and Alice-Eves links, respectively. Moreover, erf(.) is the error function [12, Eq. (8.250.1)], $u = \frac{\sqrt{\pi}a}{\sqrt{2}w_d}$, $u_m = \frac{\sqrt{\pi}a_m}{\sqrt{2}w_{d,m}}$, a is the radius of Bob's effective area, a_m is the radius of the m-th Eve's effective area, and w_d and $w_{d,m}$ are the Alice's beam footprint at a distance of d and d_m for the Bob and Eves links, respectively [2], [11].

The received signals at Bob and the m-th Eve are respectively expressed as

$$y_b = \sqrt{P_t}\alpha_b\beta\sum_{i=1}^{N} h_i e^{j\theta_i} g_i \; x + n_b, \quad (7)$$

$$y_m = \sqrt{P_t}\alpha_m\beta_m\sum_{i=1}^{N} h_i e^{j\theta_i} \mathcal{E}_{i,m} \; x + n_m, \quad (8)$$

where P_t is the transmit power, $\theta_i \in [0, 2\pi)$ is the phase shift applied by the i-th RE which is a uniformly distributed RV, x is the transmitted symbol with $\mathbb{E}[|x|^2] = 1$, and $n_b \sim \mathcal{CN}(0, \sigma_b^2)$ and $n_m \sim \mathcal{CN}(0, \sigma_m^2)$ are the additive white Gaussian noise (AWGN) at Bob and the m-th Eve, respectively.

Since Bob is an active user, its instantaneous channel state information (CSI) is assumed to be known at Alice, and thus the phases of h_i and g_i are available at the IRS [5], [13]. In addition, it is assumed that the REs apply discrete phase shifts from the set of $\mathcal{S} \triangleq \{0, \frac{2\pi}{2^q}, \ldots, \frac{2\pi(2^q-1)}{2^q}\}$, where q is the number of quantization bits [7]. Therefore, due to the discrete values of the phase shifts, the phases cannot be perfectly aligned and the legitimate communication suffers from phase shift quantization errors, i.e. $\Psi_i = \theta_i - \arg(h_i) - \arg(g_i)$, which are uniformly distributed in the interval of $[-\frac{\pi}{2^q}, \frac{\pi}{2^q}]$. Let $\gamma_t \triangleq \frac{P_t}{\sigma_b^2}$, the instantaneous SNR at Bob is expressed as

$$\gamma_b = \gamma_t\alpha_b^2\left|\beta\right|^2\left|\sum_{i=1}^{N}\left|h_i\right|\left|g_i\right|e^{j\Psi_i}\right|^2. \quad (9)$$

On the other hand, since Eves are not scheduled/active users but passive users, it is almost impossible for Alice to obtain the instantaneous CSI of Eves [14]. In addition, as the IRS does not include radio frequency chains but it works in a passive manner, the instantaneous CSI cannot be directly obtained by the IRS [13]. However, the statistical CSI of Eves is assumed to be available [9], [13], [14]. Therefore, let $\gamma_{tm} \triangleq \frac{P_t}{\sigma_m^2}$, the received SNR at the m-th Eve is expressed as

$$\gamma_m = \gamma_{tm}\alpha_m^2\left|\beta_m\right|^2\left|\sum_{i=1}^{N} h_i\mathcal{E}_{i,m}e^{j\theta_i}\right|^2. \quad (10)$$

III. Secrecy Capacity

In order to study the secrecy performance in different cases of Eves, an accurate lower bound on the secrecy capacity can be mathematically formulated as [4]

$$\begin{aligned}\mathcal{C}_s &= \Big[\mathbb{E}\left[\log_2\left(1+\gamma_b\right)\right] - \mathbb{E}\left[\log_2\left(1+\gamma_E\right)\right]\Big]^+ \\ &\triangleq \left[\mathcal{C}_b - \mathcal{C}_E\right]^+, \end{aligned} \quad (11)$$

where $[x]^+ = \max[x, 0]$, and $\mathcal{C}_b$ and $\mathcal{C}_E$ are the ergodic capacities of Bob and Eves, respectively.

A. Ergodic Capacity of Bob

The ergodic capacity of Bob is written as [4, Eq. (34)]

$$\mathcal{C}_b = \frac{1}{\ln 2}\int_0^\infty \frac{1 - F_{\gamma_b}\left(z\right)}{1+z}\mathrm{d}z, \quad (12)$$

where $F_{\gamma_b}\left(z\right)$ is the cumulative distribution function (CDF).

Since the Alice-IRS-Bob channels are non-zero mean CG RVs, their amplitudes are modelled by Rician distribution. Let $\eta \triangleq \left(\sum_{i=1}^{N} |h_i|\,|g_i| \cos\Psi_i\right)^2 + \left(\sum_{i=1}^{N} |h_i|\,|g_i| \sin\Psi_i\right)^2 \triangleq \omega_R^2 + \omega_I^2$, it can be accurately modelled by gamma distribution [5], [6], where its CDF is written as

$$F_\eta(\eta) = 1 - \frac{1}{\Gamma(\psi)}\Gamma\left(\psi, \frac{\eta}{\Omega}\right), \tag{13}$$

where $\Gamma(.)$ is the gamma function [12, Eq. (8.310)], $\Gamma(.,.)$ is the upper incomplete gamma function [12, Eq. (8.350.2)], $\psi = \mu_\eta^2/\sigma_\eta^2$ and $\Omega = \sigma_\eta^2/\mu_\eta$ with $\mu_\eta = \mathbb{E}\left[\omega_R^2\right] + \mathbb{E}\left[\omega_I^2\right]$, $\sigma_\eta^2 = \mathbb{V}\left[\omega_R^2\right] + \mathbb{V}\left[\omega_I^2\right]$, $\mathbb{E}\left[\omega_R^2\right] = \mathbb{V}[\omega_R] + \mathbb{E}^2[\omega_R]$, $\mathbb{E}\left[\omega_I^2\right] = \mathbb{V}[\omega_I] + \mathbb{E}^2[\omega_I]$, $\mathbb{E}[\omega_R] = N\mathbb{E}[|h_i|]\mathbb{E}[|g_i|]\mathcal{F}_1$, $\mathbb{E}[\omega_I] = 0$, $\mathbb{V}[\omega_R] = N\mathbb{V}[|h_i|\,|g_i|\cos\Psi_i]$, $\mathbb{V}[\omega_I] = N\mathbb{V}[|h_i|\,|g_i|\sin\Psi_i]$, $\mathbb{E}[\cos\Psi_i] = \mathcal{F}_1$, $\mathbb{E}[\sin\Psi_i] = 0$, $\mathbb{V}[\cos\Psi_i] = 1/2 + \mathcal{F}_2/2 - \mathcal{F}_1^2$, $\mathbb{V}[\sin\Psi_i] = 1/2 - \mathcal{F}_2/2$, $\mathcal{F}_1 = \frac{\sin(\pi/2^q)}{2^{-q}\pi}$, $\mathcal{F}_2 = \frac{\sin(2\pi/2^q)}{2^{-q+1}\pi}$ [6], $\mathbb{E}\left[|h_i|^\ell\right] = \sigma_{h_i}^\ell \Gamma(1+\ell/2)\, L_{\ell/2}\left(-\mu_{h_i}^2/\sigma_{h_i}^2\right)$, $\mathbb{E}\left[|g_i|^\ell\right] = \sigma_{g_i}^\ell \Gamma(1+\ell/2)\, L_{\ell/2}\left(-\mu_{g_i}^2/\sigma_{g_i}^2\right)$, $\mathbb{V}\left[\omega_R^2\right] = 2\mathbb{V}[\omega_R]\left(\mathbb{V}[\omega_R] + 2\mathbb{E}^2[\omega_R]\right)$, $\mathbb{V}\left[\omega_I^2\right] = 2\mathbb{V}^2[\omega_I]$ [15], and $L_{\ell/2}(.)$ is the Laguerre polynomial [12, Eq. (8.970.1)].

Let $\vartheta \triangleq |\beta|$, by exploiting (9) and (13), the conditional CDF of γ_b is expressed as

$$F_{\gamma_b}\left(z\middle|\vartheta\right) = 1 - \frac{1}{\Gamma(\psi)}\Gamma\left(\psi, \frac{z}{\Omega\gamma_t\alpha_b^2\vartheta^2}\right). \tag{14}$$

By applying [16, Eq. (07.34.03.0613.01)] and [12, Eq. (9.31.2)], (14) is equivalently expressed as

$$F_{\gamma_b}\left(z\middle|\vartheta\right) = 1 - \frac{1}{\Gamma(\psi)} G_{2,1}^{0,2}\left[\frac{\Omega\gamma_t\alpha_b^2}{z}\vartheta^2 \,\middle|\, \begin{matrix} 1-\psi, 1 \\ 0 \end{matrix}\right], \tag{15}$$

where $G_{p,q}^{m,n}\left[.\middle|\, .,. \,\right]$ is the MeijerG function [12, Eq. (9.301)].

In order to derive the unconditional CDF of γ_b, we take the expectation of (15) with respect to ϑ. Therefore, by exploiting (15) and (5), it is written as

$$F_{\gamma_b}(z) = 1 - \int_0^{\varphi} \frac{\xi\vartheta^{\xi-1}}{\varphi^\xi\Gamma(\psi)} G_{2,1}^{0,2}\left[\frac{\Omega\gamma_t\alpha_b^2\vartheta^2}{z} \,\middle|\, \begin{matrix} 1-\psi, 1 \\ 0 \end{matrix}\right] \mathrm{d}\vartheta. \tag{16}$$

The integral of (16) is evaluated through [16, Eq. (07.34.21.0084.01)], and it is obtained as

$$F_{\gamma_b}(z) = 1 - \frac{\xi}{2\Gamma(\psi)} G_{4,3}^{0,4}\left[\frac{\Omega\gamma_t\alpha_b^2}{z\varphi^{-2}} \,\middle|\, \begin{matrix} \frac{1-\xi}{2}, \frac{2-\xi}{2}, 1-\psi, 1 \\ 0, -\frac{\xi}{2}, \frac{1-\xi}{2} \end{matrix}\right]. \tag{17}$$

Furthermore, by applying the identities given in [12, Eq. (9.31.1)] and [12, Eq. (9.31.2)], a further simplified expression for the CDF of γ_b is obtained as

$$F_{\gamma_b}(z) = 1 - \frac{\xi}{2\Gamma(\psi)} G_{2,3}^{3,0}\left[\frac{z}{\Omega\gamma_t\alpha_b^2\varphi^2} \,\middle|\, \begin{matrix} 1, 1+\frac{\xi}{2} \\ \frac{\xi}{2}, \psi, 0 \end{matrix}\right]. \tag{18}$$

By substituting (18) into (12), $\mathcal{C}_b$ is written as

$$\mathcal{C}_b = \frac{\xi}{2\Gamma(\psi)\ln 2}\int_0^{\infty} \frac{1}{1+z} G_{2,3}^{3,0}\left[\frac{z}{\Omega\gamma_t\alpha_b^2\varphi^2} \,\middle|\, \begin{matrix} 1, 1+\frac{\xi}{2} \\ \frac{\xi}{2}, \psi, 0 \end{matrix}\right] \mathrm{d}z. \tag{19}$$

We then use [16, Eq. (07.34.21.0086.01)] to evaluate (19), and thus the ergodic capacity of Bob is obtained as

$$\mathcal{C}_b = \frac{\xi}{2\Gamma(\psi)\ln 2} G_{3,4}^{4,1}\left[\frac{1}{\Omega\gamma_t\alpha_b^2\varphi^2} \,\middle|\, \begin{matrix} 0, 1, 1+\frac{\xi}{2} \\ 0, \frac{\xi}{2}, \psi, 0 \end{matrix}\right]. \tag{20}$$

B. Ergodic Capacity of Eavesdroppers

In order to derive the ergodic capacity of Eves, we first need to derive the distribution of γ_m. Let $\mathcal{A}_m \triangleq \sum_{i=1}^{N} h_i\mathcal{E}_{i,m}e^{j\theta_i}$, where h_i and $\mathcal{E}_{i,m}$ are CG RVs, and θ_i is a uniformly distributed RV. Therefore, according to [17, Proposition 2], for a sufficiently large number of REs, it can be stated that $\mathcal{A}_m \sim \mathcal{CN}(0, N\mathcal{V}_m)$ with $\mathcal{V}_m \triangleq \left(\sigma_{h_i}^2 + \mu_{h_i}^2\right)\left(\sigma_{i,m}^2 + \mu_{i,m}^2\right)$. Moreover, $\eta_m \triangleq |\mathcal{A}_m|^2 \sim \mathrm{Exp}\left(\frac{1}{N\mathcal{V}_m}\right)$ is an exponential RV.

1) Ergodic Capacity of Colluding Eavesdroppers: We assume that all Eves cooperatively attempt to overhear the Alice-Bob information, and thus the MRC technique is used. Therefore, the end-to-end eavesdropping SNR becomes the sum of each individual Eve's SNR, i.e. $\gamma_E = \sum_{m=1}^{M}\gamma_m$. As a result, the ergodic capacity can be written as [18, Eq. (2)]

$$\mathcal{C}_E = \frac{1}{\ln 2}\int_0^{\infty} \frac{1}{z}\left[1 - \mathcal{M}_{\gamma_E}(-z)\right] e^{-z}\mathrm{d}z, \tag{21}$$

where $\mathcal{M}_{\gamma_E}(-z) = \mathbb{E}\left[e^{-z\gamma_E}\right]$ is the moment generating function (MGF) of γ_E.

It is assumed that $\gamma_m\ \forall m = 1, \ldots, M$ can be non-identical. Furthermore, the authors in [19, Appendix B] have shown that for a large number of REs, $\gamma_m\ \forall m = 1, \ldots, M$ are uncorrelated. Therefore, the MGF of γ_E is written as

$$\mathcal{M}_{\gamma_E}(-z) = \mathbb{E}\left[e^{-z\sum_{m=1}^{M}\gamma_m}\right] = \prod_{m=1}^{M}\mathbb{E}\left[e^{-z\gamma_m}\right], \tag{22}$$

where $\mathcal{M}_{\gamma_m}(-z) \triangleq \mathbb{E}\left[e^{-z\gamma_m}\right]$ is the MGF of the m-th Eve.

Let $\vartheta_m \triangleq |\beta_m|$, since η_m is an exponential RV, using (10), the conditional MGF for the m-th Eve is expressed as

$$\mathcal{M}_{\gamma_m}\left(-z\middle|\vartheta_m\right) = \frac{1}{1 + N\mathcal{V}_m\gamma_{tm}\alpha_m^2\vartheta_m^2 z}. \tag{23}$$

We then take the expectation of (23) with respect to ϑ_m. Therefore, using (6), the unconditional MGF is derived as

$$\mathcal{M}_{\gamma_m}(-z) = \frac{\xi_m}{\varphi_m^{\xi_m}}\int_0^{\varphi_m} \frac{\vartheta_m^{\xi_m-1}}{1 + N\mathcal{V}_m\gamma_{tm}\alpha_m^2\vartheta_m^2 z}\mathrm{d}\vartheta_m. \tag{24}$$

By interchange of $x_m \triangleq \vartheta_m^2$, (24) is rewritten as

$$\mathcal{M}_{\gamma_m}(-z) = \frac{\xi_m}{2\varphi_m^{\xi_m}}\int_0^{\varphi_m^2} \frac{x_m^{\frac{\xi_m}{2}-1}}{1 + N\mathcal{V}_m\gamma_{tm}\alpha_m^2 z\ x_m}\mathrm{d}x_m. \tag{25}$$

The integral of (25) is evaluated by [12, Eq. (3.194.1)] as

$$\mathcal{M}_{\gamma_m}(-z) = {}_2F_1\left(1, \frac{\xi_m}{2}; \frac{\xi_m+2}{2}; -\Xi z\right), \tag{26}$$

where $\Xi = N\mathcal{V}_m\gamma_{tm}\alpha_m^2\varphi_m^2$ and ${}_2F_1(.,.;.;.)$ is the Gauss hypergeometric function [12, Eq. (9.14.1)].

By substituting (26) into (22), the MGF of γ_E is obtained, and then by substituting (22) into (21), $\mathcal{C}_E$ is obtained as

$$\mathcal{C}_E = \int_0^{\infty} \frac{\left[1 - \prod_{m=1}^{M}\ {}_2F_1\left(1, \frac{\xi_m}{2}; \frac{\xi_m+2}{2}; -\Xi z\right)\right]}{ze^z\ln 2}\mathrm{d}z. \tag{27}$$

The integral of (27) is easily assessed by numerical integration. Moreover, using the Gauss-Laguerre integration method [20, Eq. (25.4.45)], its closed-form expression is obtained as

$$\mathcal{C}_E = \sum_{\ell=1}^{L} \frac{\left[1 - \prod_{m=1}^{M}\ {}_2F_1\left(1, \frac{\xi_m}{2}; \frac{\xi_m+2}{2}; -\Xi\chi_\ell\right)\right]}{\lambda_\ell^{-1}\chi_\ell\ln 2} + \mathcal{R}_L, \tag{28}$$

where χ_ℓ and λ_ℓ are respectively the sample points and the weights factors tabulated in [20, TABLE (25.9)], and $\mathcal{R}_L$ is a remainder which is determined as shown in [20, Eq. (25.4.45)]. However, for a large L, $\mathcal{R}_L \to 0$ and it can be neglected.

2) Ergodic Capacity of Non-Colluding Eavesdroppers: When each Eve independently attempts to overhear the Alice-Bob information, the Eve with the strongest SNR, $\gamma_E = \max[\gamma_1, \ldots, \gamma_M]$, is the most calamitous, and thus the SC technique is used [5]. Since Eves can be non-identical, and η_m is an exponential RV, by letting $\vartheta_m \triangleq |\beta_m|$ and using (10), the conditional CDF of the m-th Eve is written as

$$F_{\gamma_m}\left(z\middle|\vartheta_m\right) = 1 - \exp\left(\frac{-z}{N\mathcal{V}_m\gamma_{tm}\alpha_m^2\vartheta_m^2}\right). \quad (29)$$

Using (6), the unconditional CDF is derived as

$$F_{\gamma_m}(z) = 1 - \int_0^{\varphi_m} \frac{\exp\left(\frac{-z}{N\mathcal{V}_m\gamma_{tm}\alpha_m^2\vartheta_m^2}\right)}{\vartheta^{1-\xi_m}\xi_m^{-1}\varphi_m^{\xi_m}}\mathrm{d}\vartheta_m. \quad (30)$$

By applying [16, Eq. (07.34.03.0228.01)] and [12, Eq. (9.31.2)], (30) is equivalently written as

$$F_{\gamma_m}(z) = 1 - \int_0^{\varphi_m} \frac{G_{1,0}^{0,1}\left[\frac{N\mathcal{V}_m\gamma_{tm}\alpha_m^2\vartheta_m^2}{z}\middle|\begin{matrix}1\\-\end{matrix}\right]}{\vartheta^{1-\xi_m}\xi_m^{-1}\varphi_m^{\xi_m}}\mathrm{d}\vartheta_m. \quad (31)$$

By exploiting [16, Eq. (07.34.21.0084.01)], (31) is evaluated. After some algebraic manipulations, it is obtained as

$$F_{\gamma_m}(z) = 1 - \frac{\xi_m}{2}G_{3,2}^{0,3}\left[\frac{\Xi}{z}\middle|\begin{matrix}\frac{1-\xi_m}{2}, \frac{2-\xi_m}{2}, 1\\ -\frac{\xi_m}{2}, \frac{1-\xi_m}{2}\end{matrix}\right], \quad (32)$$

where $\Xi \triangleq N\mathcal{V}_m\gamma_{tm}\alpha_m^2\varphi_m^2$.

By applying the identities given in [12, Eq. (9.31.2] and [16, Eq. (07.34.03.0001.01)], (32) is further simplified as

$$F_{\gamma_m}(z) = 1 - \frac{\xi_m}{2}G_{1,2}^{2,0}\left[\frac{z}{\Xi}\middle|\begin{matrix}\frac{\xi_m+2}{2}\\ \frac{\xi_m}{2}, 0\end{matrix}\right]. \quad (33)$$

The CDF of $\gamma_E = \max[\gamma_1, \ldots, \gamma_M]$ is written as

$$F_{\gamma_E}(z) = \prod_{m=1}^{M}\left[1 - \tfrac{\xi_m}{2}G_{1,2}^{2,0}\left[\frac{z}{\Xi}\middle|\begin{matrix}\frac{\xi_m+2}{2}\\ \frac{\xi_m}{2}, 0\end{matrix}\right]\right]. \quad (34)$$

Similar to (12), the ergodic capacity is expressed as

$$\mathcal{C}_E = \int_0^{\infty} \frac{1 - \prod_{m=1}^{M}\left[1 - \frac{\xi_m}{2}G_{1,2}^{2,0}\left[\frac{z}{\Xi}\middle|\begin{matrix}\frac{\xi_m+2}{2}\\ \frac{\xi_m}{2}, 0\end{matrix}\right]\right]}{\ln 2\ (1+z)}\mathrm{d}z. \quad (35)$$

In addition, using [20, Eq. (25.4.45)], a closed-form expression for (35) can be written in terms of the weights factors and sample points of the Laguerre orthogonal polynomial as

$$\mathcal{C}_E = \sum_{\ell=1}^{L} \frac{1 - \prod_{m=1}^{M}\left[1 - \frac{\xi_m}{2}G_{1,2}^{2,0}\left[\frac{\chi_\ell}{\Xi}\middle|\begin{matrix}\frac{\xi_m+2}{2}\\ \frac{\xi_m}{2}, 0\end{matrix}\right]\right]}{\ln 2\ (1+\chi_\ell)\,\lambda_\ell^{-1}e^{-\chi_\ell}} + \mathcal{R}_L, \quad (36)$$

where $\mathcal{R}_L$ is determined as shown in [20, Eq. (25.4.45)], however, for a large L, it becomes negligible. Moreover, χ_ℓ are the sample points and λ_ℓ are the weights factors, tabulated in [20, TABLE (25.9)].

Finally, by substituting (20) and (28)/(36) into (11), the secrecy capacity with colluding/non-colluding Eves is obtained.

C. Asymptotic Analysis

In order to gain further insights into the secrecy performance, the asymptotic secrecy capacity in the presence of independent but not necessarily identical colluding Eves can be written as

$$\hat{\mathcal{C}}_s = \left[\log_2\left(\frac{\left[(N-1)\mu^2 + \bar{\mu}\right]\mathcal{X}}{\sum_{m=1}^{M}\mathcal{V}_m\alpha_m^2\mathbb{E}\left[\vartheta_m^2\right]}\right) - \mathcal{A} + \mathcal{B}\right]^+, \quad (37)$$

where $\mu = \mathbb{E}[|h_i|\,|g_i|]\mathcal{F}_1$, $\bar{\mu} = \mathbb{E}[|h_i|^2\,|g_i|^2]$, $\mathcal{X} = \alpha_b^2\mathbb{E}\left[\vartheta^2\right]$, $\mathcal{A} = \frac{\mathbb{E}\left[\vartheta^4\right](1/\psi+1)}{2\mathbb{E}^2[\vartheta^2]} - \frac{1}{2}$, and $\mathcal{B} = \frac{\sum_{m=1}^{M}\mathcal{V}_m^2\alpha_m^4\left(2\mathbb{E}\left[\vartheta_m^4\right] - \mathbb{E}^2\left[\vartheta_m^2\right]\right)}{2\left(\sum_{m=1}^{M}\mathcal{V}_m\alpha_m^2\mathbb{E}[\vartheta_m^2]\right)^2}$.

Proof: For $\gamma_t = \gamma_{tm} \to \infty$, we can write that $\hat{\mathcal{C}}_s = \left[\mathbb{E}\left[\log_2\left(\frac{1+\gamma_t\mathcal{G}_b}{1+\gamma_t\mathcal{G}_E}\right)\right]\right]^+ = \left[\mathbb{E}\left[\log_2\left(\frac{\mathcal{G}_b}{\mathcal{G}_E}\right)\right]\right]^+ = \left[\mathbb{E}\left[\log_2(\mathcal{G}_b)\right] - \mathbb{E}\left[\log_2(\mathcal{G}_E)\right]\right]^+$. In addition, using the second-order Taylor expansion and Gaussian approximation for $\mathbb{E}[x]$, it can be written that $\mathbb{E}\left[\log_2(x)\right] \approx \log_2\left(\mathbb{E}[x]\right) - \frac{\mathbb{V}[x]}{2\mathbb{E}^2[x]}$ [21]. Therefore, for a sufficiently large number of REs, $\hat{\mathcal{C}}_s = \left[\log_2\left(\frac{\mathbb{E}[\mathcal{G}_b]}{\mathbb{E}[\mathcal{G}_b]}\right) - \frac{\mathbb{V}[\mathcal{G}_b]}{2\mathbb{E}^2[\mathcal{G}_b]} + \frac{\mathbb{V}[\mathcal{G}_E]}{2\mathbb{E}^2[\mathcal{G}_E]}\right]^+$, where $\mathbb{E}\left[\mathcal{G}_b\right] = \mathbb{E}\left[\alpha_b^2\vartheta^2\eta\right] = \alpha_b^2\mathbb{E}\left[\vartheta^2\right]\mu_\eta$, $\mathbb{E}\left[\mathcal{G}_b^2\right] = \alpha_b^4\mathbb{E}\left[\vartheta^4\right]\mathbb{E}\left[\eta^2\right]$, $\mathbb{E}\left[\mathcal{G}_E\right] = \sum_{m=1}^{M}\alpha_m^2\mathbb{E}\left[\vartheta_m^2\right]\mathbb{E}\left[\eta_m\right]$, $\mathbb{E}\left[\eta_m\right] = N\mathcal{V}_m$, $\mathbb{V}\left[\eta_m\right] = N^2\mathcal{V}_m^2$, $\mathbb{V}\left[\mathcal{G}_E\right] = \sum_{m=1}^{M}\alpha_m^4N^2\mathcal{V}_m^2\left(2\mathbb{E}\left[\vartheta_m^4\right] - \mathbb{E}^2\left[\vartheta_m^2\right]\right)$, $\mathbb{E}\left[\vartheta^\ell\right] = \frac{\xi\varphi^\ell}{\xi+\ell}$ and $\mathbb{E}\left[\vartheta_m^\ell\right] = \frac{\xi_m\varphi_m^\ell}{\xi_m+\ell}$ [11, Eq. (A-2)]. Moreover, let $\mathcal{A} \triangleq \frac{\mathbb{V}[\mathcal{G}_b]}{2\mathbb{E}^2[\mathcal{G}_b]} = \frac{\mathbb{E}[\mathcal{G}_b^2]}{2\mathbb{E}^2[\mathcal{G}_b]} - \frac{1}{2}$ and $\mathcal{B} \triangleq \frac{\mathbb{V}[\mathcal{G}_E]}{2\mathbb{E}^2[\mathcal{G}_E]}$, by substituting the corresponding mean and variance terms from (13), the asymptotic secrecy capacity given in (37) is obtained. ■

Remark 1. *From (37), it is evident that the asymptotic secrecy capacity is independent of SNR, which indicates that it reaches a limit, where the limit is scaled with N.*

IV. Numerical and Simulation Results

In order to numerically assess the secrecy capacity and verify the accuracy of the expressions, we provide numerical and simulation results by setting $c = 3 \times 10^8$ m/sec, $f = 0.3$ THz, $G_t = G_b = G_m = 40$ dBi, $\frac{w_d}{a} = \frac{w_{d,m}}{a_m} = 6$, $\sigma = \sigma_m = 0.01$ m, $\phi = 50\%$, $T = 27^oC$, $\rho = 101325$ Pa [2], [11], $M = 4$, $N = \{100, 200\}$, $\sigma_{h_i}^2 = \sigma_{g_i}^2 = \sigma_{i,m}^2 = 1$, $\mu_{h_i} = \mu_{g_i} = 3$, $\mu_{i,1} = \mu_{i,2} = 1$, $\mu_{i,3} = \mu_{i,4} = 0$, $d_1 = d_2 = 10$ m, $d_{2,1} = 15$ m, $d_{2,2} = 20$ m, $d_{2,3} = 25$ m, $d_{2,4} = 30$ m, and $q = \{1, 2\}$ bits.

Fig. 1 and Fig. 2 illustrate the secrecy capacity versus SNR in the presence of colluding and non-colluding Eves, respectively. Since the numerical and simulation results are in a good agreement, the accuracy of the expressions given in (20), (27) and (35) is validated. Both figures show three different scenarios; the worst case scenario where only Bob suffers from PE, the best case scenario where only Eves suffer from PE, and the more realistic scenario where both Bob and Eves suffer from PE. The figures show the significant impacts of PE on the secrecy capacity, which cannot be neglected. Moreover, as shown in Fig. 1, in the high-SNR regime, the secrecy capacity reaches a limit, which confirms Remark 1 and (37). Furthermore, according to (9) and (10), by increasing N, the SNRs of Bob and Eves are increased. However, since the phases of IRS-Eves channels are not known at the IRS, the improvements in the SNR of Bob are much more compared

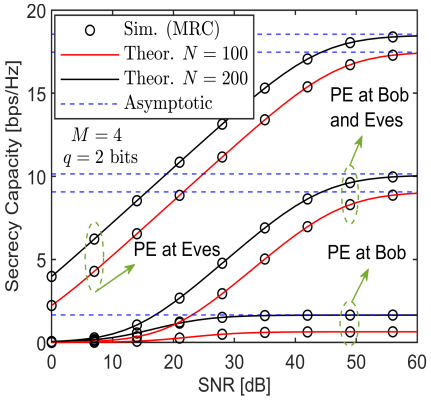

Fig. 1 Secrecy capacity in the presence of colluding Eves.

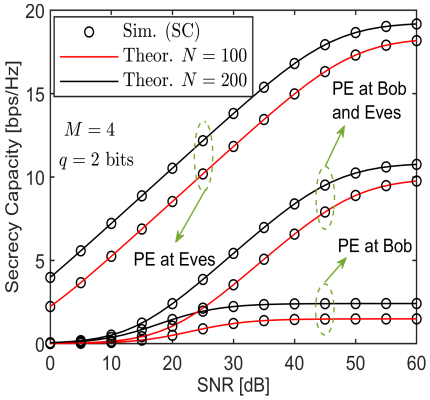

Fig. 2 Secrecy capacity in the presence of non-colluding Eves.

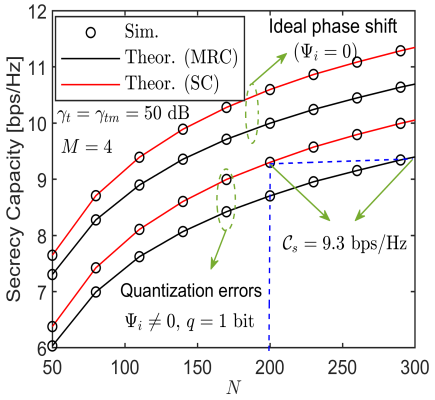

Fig. 3 Effects of colluding and non-colluding Eves, and quantization errors.

to those of the Eves, and thus it improves the system security. For example, as shown in the figures, the secrecy capacity and the asymptotic limits are improved by increasing N from 100 to 200, which confirms that an IRS not only improves the overall performance but also the PLS of THz systems.

Fig. 3 depicts a comparison between the colluding and non-colluding Eves versus the number of REs for $M = 4$ and $\gamma_t = \gamma_{tm} = 50$ dB, where both Bob and Eves suffer from PE. It also shows a comparison between the ideal and non-ideal phase shifts (i.e. $\Psi_i = 0$ and $\Psi_i \neq 0$), where in both types of Eves, the phase shifts obtained with a one-bit phase shift quantizer significantly impact the PLS. Moreover, it is shown that colluding Eves severely impact the PLS. For example, the system with quantization errors ($\Psi_i \neq 0$) and non-colluding Eves achieves a secrecy capacity of 9.3 bps/Hz with $N = 200$, while in the case of colluding Eves, it achieves the same secrecy capacity with almost $N = 300$.

V. Conclusion

In this letter, we considered an IRS-assisted THz wireless system suffering from pointing errors, phase errors and multiple Eves. By taking the colluding and non-colluding Eves into account, we extracted new expressions for the secrecy capacity, which were verified by Monte-Carlo simulations. The adverse effects of pointing errors, quantization errors and colluding Eves on the physical layer security of THz systems were analyzed, which cannot be neglected. In addition, it was shown that in the high-SNR regime, the secrecy capacity reaches a limit, which is scaled with the number of reflecting elements.

References

[1] V.-L. Nguyen, P.-C. Lin, B.-C. Cheng, R.-H. Hwang, and Y.-D. Lin, "Security and privacy for 6G: A survey on prospective technologies and challenges," *IEEE Commun. Surveys Tuts.*, vol. 23, no. 4, pp. 2384–2428, 4th Quart. 2021.

[2] A.-A. A. Boulogeorgos, E. N. Papasotiriou, and A. Alexiou, "Analytical performance assessment of THz wireless systems," *IEEE Access*, vol. 7, pp. 11 436–11 453, Jan. 2019.

[3] L. Yang, J. Yang, W. Xie, M. O. Hasna, T. Tsiftsis, and M. D. Renzo, "Secrecy performance analysis of RIS-aided wireless communication systems," *IEEE Trans. Veh. Technol.*, vol. 69, no. 10, pp. 12 296–12 300, Oct. 2020.

[4] K. Cao, H. Ding, W. Li, L. Lv, M. Gao, F. Gong, and B. Wang, "On the ergodic secrecy capacity of intelligent reflecting surface aided wireless powered communication systems," *IEEE Wireless Commun. Lett.*, vol. 11, no. 11, pp. 2275–2279, Nov. 2022.

[5] L. Wei, K. Wang, C. Pan, and M. Elkashlan, "Secrecy performance analysis of RIS-aided communication system with randomly flying eavesdroppers," *IEEE Wireless Commun. Lett.*, vol. 11, no. 10, pp. 2240–2244, Oct. 2022.

[6] A. M. Tota Khel and K. A. Hamdi, "Effects of hardware impairments on IRS-enabled MISO wireless communication systems," *IEEE Commun. Lett.*, vol. 26, no. 2, pp. 259–263, Feb. 2022.

[7] J. Qiao and M.-S. Alouini, "Secure transmission for intelligent reflecting surface-assisted mmWave and terahertz systems," *IEEE Wireless Commun. Lett.*, vol. 9, no. 10, pp. 1743–1747, Oct. 2020.

[8] B. Ning, Z. Chen, W. Chen, and L. Li, "Improving security of THz communication with intelligent reflecting surface," in *Proc. IEEE Globecom Workshops (GC Wkshps)*, Waikoloa, HI, USA, Dec. 2019, pp. 1–6.

[9] J. Qiao, C. Zhang, A. Dong, J. Bian, and M.-S. Alouini, "Securing intelligent reflecting surface assisted terahertz systems," *IEEE Trans. Veh. Technol.*, vol. 71, no. 8, pp. 8519–8533, Aug. 2022.

[10] Y. Pan, K. Wang, C. Pan, H. Zhu, and J. Wang, "Sum-rate maximization for intelligent reflecting surface assisted terahertz communications," *IEEE Trans. Veh. Technol.*, vol. 71, no. 3, pp. 3320–3325, Mar. 2022.

[11] H. Du, J. Zhang, K. Guan, D. Niyato, H. Jiao, Z. Wang, and T. Kurner, "Performance and optimization of reconfigurable intelligent surface aided THz communications," *IEEE Trans. Commun.*, vol. 70, no. 5, pp. 3575–3593, May 2022.

[12] I. S. Gradshteyn and I. M. Ryzhik, *Table of Integrals, Series, and Products*, 8th ed. Oxford, UK: Academic Press: Elsevier, 2014.

[13] X. Yu, D. Xu, Y. Sun, D. W. K. Ng, and R. Schober, "Robust and secure wireless communications via intelligent reflecting surfaces," *IEEE J. Select. Areas Commun.*, vol. 38, no. 11, pp. 2637–2652, Nov. 2020.

[14] J. Liu, J. Zhang, Q. Zhang, J. Wang, and X. Sun, "Secrecy rate analysis for reconfigurable intelligent surface-assisted MIMO communications with statistical CSI," *China Commun.*, vol. 18, no. 3, pp. 52–62, Mar. 2021.

[15] A. M. Tota Khel and K. A. Hamdi, "Performance analysis of IRS-assisted full-duplex wireless communication systems with interference," *IEEE Commun. Lett.*, vol. 26, no. 9, pp. 2027–2031, Sep. 2022.

[16] Wolfram Research. (2001). *The Wolfram Functions Site: Meijer G-Function*. [Online]. Available: https://functions.wolfram.com/PDF/MeijerG.pdf

[17] J. Lyu and R. Zhang, "Hybrid active/passive wireless network aided by intelligent reflecting surface: System modeling and performance analysis," *IEEE Trans. Wireless Commun.*, vol. 20, no. 11, pp. 7196–7212, Nov. 2021.

[18] K. A. Hamdi, "A useful lemma for capacity analysis of fading interference channels," *IEEE Trans. Commun.*, vol. 58, no. 2, pp. 411–416, Feb. 2010.

[19] X. Gan, C. Zhong, Y. Zhu, and Z. Zhong, "User selection in reconfigurable intelligent surface assisted communication systems," *IEEE Commun. Lett.*, vol. 25, no. 4, pp. 1353–1357, Apr. 2021.

[20] M. Abramowitz and I. A. Stegun, *Handbook of Mathematical Functions with Formulas, Graphs, and Mathematical Tables*, 10th ed. New York, NY, USA: Dover, 1972.

[21] Y. Teh, D. Newman, and M. Welling, "A collapsed variational Bayesian inference algorithm for latent Dirichlet allocation," in *Proc. Adv. Neural Inf. Process. Syst.*, Vancouver, British Columbia, Canada, Dec. 2006, p. 353–1360.